Machine-learning-based models assist the prediction of pulmonary embolism in autoimmune diseases: A retrospective, multicenter study

Ziwei Hu[1], Yangyang Hu[1], Shuoqi Zhang[2], Li Dong[3], Xiaoqi Chen[4], Huiqin Yang[5], Linchong Su[6], Xiaoqiang Hou[7], Xia Huang[6], Xiaolan Shen[7], Cong Ye[1], Wei Tu[1], Yu Chen[1], Yuxue Chen[1], Shaozhe Cai[1], Jixin Zhong[1], Lingli Dong[1]

[1]Department of Rheumatology and Immunology, Tongji Hospital, Tongji Medical College, Huazhong University of Science and Technology, Wuhan, Hubei 430030, China;
[2]Department of Radiology, Tongji Hospital, Tongji Medical College, Huazhong University of Science and Technology, Wuhan, Hubei 430030, China;
[3]Department of Rheumatology and Immunology, Jingzhou Central Hospital, Yangtze University, Jinzhou, Hubei 434020, China;
[4]Department of Rheumatology and Immunology, Zhongnan Hospital, Wuhan University, Wuhan, Hubei 430071, China;
[5]Department of Rheumatology, Wuhan No.1 Hospital, Wuhan, Hubei 430022, China;
[6]Department of Rheumatology, Minda Hospital of Hubei Minzu University, Enshi, Hubei 445000, China;
[7]Department of Rheumatology and Immunology, The First College of Clinical Medical Science, China Three Gorges University, Yichang, Hubei 443003, China.

Abstract

Background: Pulmonary embolism (PE) is a severe and acute cardiovascular syndrome with high mortality among patients with autoimmune inflammatory rheumatic diseases (AIIRDs). Accurate prediction and timely intervention play a pivotal role in enhancing survival rates. However, there is a notable scarcity of practical early prediction and risk assessment systems of PE in patients with AIIRD.

Methods: In the training cohort, 60 AIIRD with PE cases and 180 age-, gender-, and disease-matched AIIRD non-PE cases were identified from 7254 AIIRD cases in Tongji Hospital from 2014 to 2022. Univariable logistic regression (LR) and least absolute shrinkage and selection operator (LASSO) were used to select the clinical features for further training with machine learning (ML) methods, including random forest (RF), support vector machines (SVM), neural network (NN), logistic regression (LR), gradient boosted decision tree (GBDT), classification and regression trees (CART), and C5.0 models. The performances of these models were subsequently validated using a multicenter validation cohort.

Results: In the training cohort, 24 and 13 clinical features were selected by univariable LR and LASSO strategies, respectively. The five ML models (RF, SVM, NN, LR, and GBDT) showed promising performances, with an area under the receiver operating characteristic (ROC) curve (AUC) of 0.962–1.000 in the training cohort and 0.969–0.999 in the validation cohort. CART and C5.0 models achieved AUCs of 0.850 and 0.932, respectively, in the training cohort. Using D-dimer as a pre-screening index, the refined C5.0 model achieved an AUC exceeding 0.948 in the training cohort and an AUC above 0.925 in the validation cohort. These results markedly outperformed the use of D-dimer levels alone.

Conclusion: ML-based models are proven to be precise for predicting the onset of PE in patients with AIIRD exhibiting clinical suspicion of PE.

Trial Registration: Chictr.org.cn: ChiCTR2200059599.

Keywords: Autoimmune inflammatory rheumatic diseases; Pulmonary embolism; Predictive model; Machine learning

Introduction

Pulmonary embolism (PE) is a lethal cardiovascular disorder caused by the sudden occlusion of arteries within the lungs, requiring prompt diagnosis and intervention. In the absence of timely and effective treatment, patients can rapidly deteriorate into a critical state with a heightened risk of fatality. The estimated overall mortality rate of acute PE could be up to 15% in the first 3 months after diagnosis,[1,2] which ranks very high among the causes of cardiovascular mortality.[3] Enhancing survival in patients with PE depends on both early and precise prediction, coupled with aggressive PE management. However, the clinical manifestations of PE, such as dyspnea, chest pain, hemoptysis, and syncope, are non-specific and heterogeneous, often mirroring symptoms observed in severe pneumonia, chronic obstructive pulmonary disease, myocardial infarction, and other conditions. While

Access this article online

Quick Response Code:

Website: www.cmj.org

DOI: 10.1097/CM9.0000000000003025

Ziwei Hu and Yangyang Hu contributed equally to this work.

Correspondence to: Lingli Dong, Jixin Zhong, Shaozhe Cai, Department of Rheumatology and Immunology, Tongji Hospital, Tongji Medical College, Huazhong University of Science and Technology, Wuhan, Hubei 430030, China
E-Mail: tjhdongll@163.com; zhongjixin620@163.com; 540361903@qq.com

Chinese Medical Journal 2024;137(15)
Received: 02-12-2023; **Online:** 12-06-2024 **Edited by:** Lishao Guo

pulmonary angiography remains the gold standard for PE diagnosis, computed tomography pulmonary angiography (CTPA) offers excellent accuracy and is an important diagnostic tool for suspected PE.[4,5] However, for acute critical patients, the potential risks associated with moving outside the ward for diagnostic examinations, such as the risk of sudden death and unforeseen adverse events, pose significant concerns. Therefore, achieving timely and accurate prediction of PE remains a challenge in clinical settings.

Autoimmune inflammatory rheumatic diseases (AIIRDs) are heterogeneous autoimmune diseases with the potential to affect multiple organs, including systemic lupus erythematosus (SLE), rheumatoid arthritis (RA), Sjögren's syndrome (SS), systemic sclerosis (SSc), etc. Several studies have indicated that AIIRDs were associated with a substantially increased risk of PE.[6–12] However, these studies primarily investigated the risk factors of PE in AIIRD patients, which cannot provide an operational algorithm helping predict the PE occurrence in AIIRD patients.

Machine learning (ML), an emerging branch of artificial intelligence, is adept at discerning the accurate statistical patterns within extensive sets of clinical features derived from recorded cases.[13] In contrast to traditional statistical methods that provide insights from observed differences among groups based on collected clinical features, ML excels in uncovering intricate relationships among various features, facilitating precise classification.[13–15] Research has revealed the immense potential of ML algorithms in the medical field, including the rapid diagnosis, risk assessment, and prognosis prediction.[14,16–20] Considering the acute and life-threatening characteristics of PE, as well as the requirement for early and precise diagnosis, ML algorithms may provide new opportunities to achieve the aforementioned aims.

To date, no study about the application of ML in the prediction or stratification of PE in AIIRD patients has been reported. In this study, we applied several ML models, and all of these models can be applied to classification tasks in the field of medicine: support vector machines (SVMs) can help find a hyperplane that maximally separates the different classes in the data; logistic regression (LR) can estimate the probability of an event occurring, of which the coefficient is commonly estimated via maximum likelihood estimation; neural network (NN) is a mathematical model similar to the structure of the human brain's neural networks, which can deliver the most optimal results by segregating data to the deepest level intended; gradient boosted decision tree (GBDT), random forest (RF), classification and regression trees (CART), and C5.0 are decision tree models, in which each question can be represented as a node, and finally create a hierarchy (GBDT and RF can show better performance; however, their algorithms are complicated, and the performers need the help of computer systems).[21,22] Here, we aimed to build risk prediction models for PE using various ML methods based on the clinical information (without the results of CTPA) recorded before PE diagnosis in AIIRD patients and validate their performances on multicentric data. Besides ML models, for which the prediction needs the assistance of computers, we also applied the ML method to develop decision trees, enabling a simple and convenient prediction of PE occurrence in our current clinical work-up.

Methods

Study design and patients

In this study, we identified a total of 60 AIIRD patients with PE (AIIRD PE) from 7254 patients with AIIRD hospitalized in Tongji Hospital from 2014 to 2022. A total of 180 age-, gender,- and disease-matched AIIRD patients without PE (AIIRD non-PE) from Tongji hospital were included as control. The information of other 41 AIIRD PE cases from Zhongnan Hospital Affiliated to Wuhan University, Jingzhou Central Hospital, Hubei University for Nationalities Affiliated Hospital, and Yichang Central People's Hospital was also collected for model validation [Figure 1A]. The detailed inclusion and exclusion criteria were recorded in Supplementary Table 1, http://links.lww.com/CM9/B902. All AIIRD PE patients included in this study were diagnosed via CTPA. This study was approved by the Institutional Ethics Committee of Tongji Hospital with informed consent waived (No. TJ-IRB20211256) and registered in the Chinese Clinical Trial Register (ChiCTR2200059599).

Data collection

Deidentified data of the enrolled patients, including their demographic (e.g., age, gender), clinical (e.g., symptoms and signs, medical history, complications, and disease outcome), and laboratory information (e.g., blood routine, coagulation function, hepatic/renal function, high sensitivity C reactive protein, erythrocyte sedimentation rate, etc.), results of examinations (e.g., CTPA and ultrasonic detection of lower extremities), and therapeutic interventions before (the nearest detection before PE diagnosis or baseline data) were extracted from the electronic medical records systems. The normal ranges and units of the laboratory indices and definitions/details of some nomenclatures (e.g., hyperlipidemia, anti-coagulant/thrombotic treatment, etc.) are recorded in Supplementary Table 2, http://links.lww.com/CM9/B902. All the laboratory, radiologic, and ultrasonic results have been independently checked and evaluated by two experts, and all of these examinations applied the standardized methods.

Model development and statistical analysis

For the development of the predictive models, we trained 7 ML models, including LR, SVM, GBDT, NN, RF, CART, and C5.0 model, with the baseline data of 60 AIIRD PE patients and 180 age-, gender-, and disease-matched (via PSM) AIIRD non-PE patients in Tongji Hospital (training cohort). Features for the model training were selected via two strategies: least absolute shrinkage and selection operator (LASSO) (lambda.1se was applied) and univariate LR (features with P <0.05), which were realized with R package "glmnet" and "stats", respectively. For the model validation, the information of 41 PE patients from other centers and the aforementioned 180 controls were applied

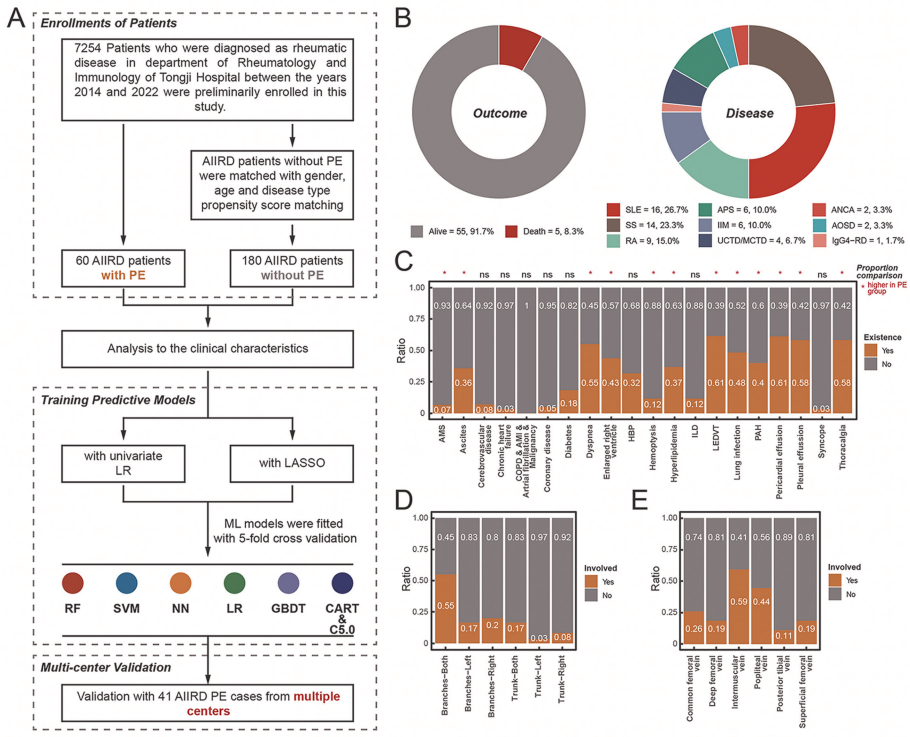

Figure 1: Study design and demographic characteristics of AIIRD with PE patients enrolled in training cohort. (A) A total number of 7254 AIIRD patients was admitted to Tongji Hospital from 2014 to 2022. Only 0.827% (60/7254) of AIIRD patients were diagnosed with PE. After matching with gender, age, and disease type, 180 AIIRD patients without PE were selected as control. These 240 patients were enrolled in the training cohort. Clinical characteristics selected by univariate LR and LASSO were applied as input of ML models (RF, SVM, NN, LR, GBDT, CART, and C5.0). And these ML models were validated by multicenter data. (B) 8.3% (5/60) of AIIRD patients with PE were dead. These 60 patients consisted of 16 SLE, 14 SS, 9 RA, 6 IIM, 6 APS, 4 UCTD/MCTD, 2 AOSD, 2 ANCA associated vasculitis, and 1 IgG4-RD. (C) Complication of these 60 AIIRD with PE patients. (D) Pattern of the exact sites of PE identified by pulmonary CTPA in 60 AIIRD with PE patients. (E) Location of LEDVT in 27 AIIRD patients with PE. AIIRD: Autoimmune inflammatory rheumatic disease; AMI: Acute myocardial infarction; AMS: Abnormal mental state; ANCA: Anti-neutrophil cytoplasmic antibodies; AOSD: Adult-onset Still disease; APS: Antiphospholipid antibody syndrome; CART: Classification and Regression Trees model; COPD: Chronic obstructive pulmonary disease; CTPA: Computed tomography pulmonary angiography; GBDT: Gradient boosted decision tree; HBP: High blood pressure; IgG: Immunoglobulin G; IgG4-RD: IgG4 related disease; IIM: Idiopathic inflammatory myopathies; ILD: Interstitial lung disease; LASSO: Least absolute shrinkage and selection operator; LEDVT: Lower extremity deep vein thrombosis; LR: Logistic regression; MCTD: Mixed connective tissue disease; ML: Machine learning; NN: Neural network; PAH: Pulmonary arterial hypertension; PE: Pulmonary embolism; RA: Rheumatoid arthritis; RF: Random forest; SLE: Systemic lupus erythematosus; SS: Sjogren's syndrome; SVM: Support vector machine; UCTD: Undifferentiated connective tissue disease.

to validate the performance of trained models (multicentric validation cohort or validation cohort). The training cohort was also applied to make the internal validation of the trained models. The training of LR, SVM, RF, GBDT, NN, and CART models was realized with method "bayesglm", "svmLinear", "rf", "gbm", "avNNet", and "rpart2" in R package "caret" with default settings, respectively, and five-fold cross-validations were applied to fine-tune the parameters. The C5.0 model was trained with C5.0 function in R package "C50." The relative feature-importance scores of the LR, RF, GBDT, and NN models were obtained via "varImp" function encapsulated in "caret". As the SVM model has no built-in importance score, the area under the ROC curve (AUC) of each selected feature was utilized to calculate their corresponding importance scores. The models' predictive performances on different datasets were evaluated by the AUC. The calculations of and the comparisons between different AUCs were realized with R package "pROC".

Chi-squared or Fisher exact tests were applied for the analysis of categorical data. Mann-Whitney *U* test were used to compare the continuous variables. Both of them were realized with R package "tableone". $P < 0.05$ (two-tailed) was considered as statistically significant. Data imputation was realized with the RF method in R package "mice". R package "ggplot2" was applied to draw plots, and all the analyses in this study were realized with R (version 4.1.1, R Foundation for Statistical Computing, Vienna, Austria).

Results

Demographic and clinical characteristics of patients with AIIRD and PE

Among these 60 AIIRD PE patients in the training cohort, 26.7% (n = 16) of them had SLE and 23.3% (n = 14) were secondary to SS, accounting for the majority of all AIIRD PE cases [Figure 1B and Supplementary Table 3, http://links.lww.com/CM9/B902]. Despite treatment, five patients succumbed to PE. The presence of lower extremity deep venous thrombosis (LEDVT), pericardial effusion, pleural effusion, thoracalgia, dyspnea, lung infection, enlarged right ventricle (RV), pulmonary arterial hypertension (PAH), hyperlipidemia, hemoptysis, ascites, and abnormal mental state (AMS) was more common in AIIRD PE patients [Figure 1C]. Comparisons of other clinical laboratory indices between PE and non-PE AIIRD

Table 1: Basic information and laboratory characteristics between AIIRD patients with and without PE in the training cohort.

Items	Without PE ($n = 180$)	With PE ($n = 60$)	χ^2/U	*P* values
Basic information				
Gender (male), *n* (%)	39 (21.7)	13 (21.7)	0.000	1.000
Age (years)	51.00 [33.00, 62.00]	51.00 [35.50, 65.00]	5304.0	0.837
Smoking, *n* (%)	16 (8.9)	7 (11.7)	0.144	0.704
Alcohol, *n* (%)	10 (5.6)	3 (5.0)	0.000	1.000
Death, *n* (%)	3 (1.7)	5 (8.3)	4.310	0.038
*Anticoagulative/thrombotic usage, *n* (%)	9 (5.0)	1 (1.7)	0.557	0.456
Laboratory parameters				
WBC ($\times 10^9$/L)	5.67 [4.32, 7.91]	7.77 [5.20, 10.40]	3977.5	0.004
Neu ($\times 10^9$/L)	3.70 [2.62, 5.92]	5.70 [2.92, 7.83]	4089.0	0.008
Hemoglobin (g/L)	118.00 [104.75, 128.00]	117.00 [97.00, 133.50]	5255.0	0.905
PLT ($\times 10^9$/L)	210.50 [148.50, 278.25]	173.00 [99.50, 265.00]	6300.0	0.032
ESR (mm/1h)	23.00 [12.00, 47.00]	27.00 [8.75, 52.50]	5082.0	0.774
hsCRP (mg/L)	2.48 [0.53, 11.54]	15.95 [5.27, 73.72]	2412.0	<0.001
IgG (g/L)	13.65 [11.09, 19.19]	12.03 [9.30, 16.04]	4835.0	0.012
C3 (g/L)	0.96 [0.78, 1.12]	0.84 [0.66, 1.16]	4514.0	0.142
C4 (g/L)	0.20 [0.14, 0.27]	0.17 [0.13, 0.21]	4767.0	0.039
PCT (ng/mL)	0.05 [0.05, 0.08]	0.11 [0.06, 0.75]	589.5	0.003
BNP (pg/mL)	119.00 [57.25, 316.50]	1364.00 [154.50, 4143.75]	582.5	<0.001
Fibrinogen (g/L)	3.32 [2.72, 4.48]	3.83 [2.80, 5.29]	4662.0	0.217
D-dimer (μg/mL)	0.63 [0.28, 1.40]	4.36 [2.26, 7.51]	1331.0	<0.001
AST (U/L)	24.00 [17.00, 37.00]	24.00 [17.50, 41.00]	4993.0	0.491
ALT (U/L)	19.00 [12.75, 35.25]	24.00 [16.00, 37.50]	4262.0	0.023
LDH (U/L)	214.50 [174.75, 284.25]	310.00 [245.00, 444.00]	1961.5	<0.001
ALP (U/L)	70.00 [55.00, 85.00]	80.00 [60.00, 98.00]	3853.5	0.034
Albumin (g/L)	40.25 [35.50, 43.12]	33.80 [30.70, 38.30]	7905.0	<0.001
Globulin (g/L)	32.25 [28.87, 37.10]	33.60 [26.40, 37.35]	5467.0	0.733
TG (mmol/L)	1.52 [1.00, 2.20]	1.62 [1.05, 2.21]	3150.5	0.591
TC (mmol/L)	3.87 [3.27, 4.53]	3.98 [3.29, 4.78]	4662.0	0.553
BUN (mmol/L)	4.90 [3.90, 6.15]	5.50 [3.91, 6.72]	4670.5	0.183
Cr (μmol/L)	59.00 [50.00, 73.50]	66.00 [53.50, 81.50]	4452.0	0.071
eGFR (mL/min per 1.73 m^2)	101.80 [88.20, 114.15]	92.30 [71.20, 109.72]	5916.0	0.050
Glucose (mmol/L)	5.95 [5.01, 6.88]	6.23 [5.27, 8.01]	3283.0	0.144
Urine protein, *n* (%)	44 (24.7)	23 (46.0)	7.659	0.006
Urine protein-24h, *n* (%)	36 (31.6)	10 (76.9)	8.669	0.004
COMBS, *n* (%)	44 (35.5)	4 (36.4)	0.000	1.000
pANCA, *n* (%)	10 (9.1)	2 (6.7)	0.003	0.958
cANCA, *n* (%)	3 (2.7)	0	0.041	0.839
anti-MPO, *n* (%)	7 (6.4)	2 (6.9)	0.000	1.000
anti-PR3, *n* (%)	1 (0.9)	0	0.000	1.000
ANA, *n* (%)	148 (86.5)	44 (80.0)	0.931	0.335
anti-u1nRNP, *n* (%)	29 (17.3)	7 (13.7)	0.145	0.703
anti-Sm, *n* (%)	18 (10.7)	4 (7.7)	0.137	0.711
anti-SSA, *n* (%)	78 (46.2)	29 (55.8)	1.112	0.292
anti-SSB, *n* (%)	41 (24.4)	7 (13.5)	2.183	0.140
anti-Ro52, *n* (%)	72 (42.4)	23 (44.2)	0.006	0.937
anti-Jo1, *n* (%)	6 (3.6)	5 (9.6)	1.914	0.167
anti-dsDNA, *n* (%)	22 (13.1)	4 (7.4)	0.788	0.375
anti-rRNP, *n* (%)	17 (10.1)	6 (11.8)	0.006	0.940
anti-Scl-70, *n* (%)	5 (3.0)	4 (7.7)	1.210	0.271
AHA, *n* (%)	10 (6.0)	1 (1.9)	0.642	0.423
anti-CENP-B, *n* (%)	8 (4.7)	3 (5.8)	0.000	1.000
ANuA, *n* (%)	13 (7.7)	4 (7.5)	0.000	1.000
β2GP1-IgA, *n* (%)	11 (7.8)	1 (3.1)	0.308	0.579
β2GP1-IgG, *n* (%)	21 (14.9)	4 (12.5)	0.005	0.945
β2GP1-IgM, *n* (%)	5 (3.5)	0	0.247	0.619
ACA-IgA, *n* (%)	10 (7.1)	4 (13.8)	0.680	0.410
ACA-IgG, *n* (%)	18 (12.8)	7 (14.9)	0.015	0.901

(*Continued*)

Table 1
(Continued)

Items	Without PE ($n = 180$)	With PE ($n = 60$)	χ^2/U	*P* values
ACA-IgM, *n* (%)	5 (3.5)	1 (2.2)	0.000	1.000
LAC, *n* (%)	29 (20.9)	12 (31.6)	1.370	0.242
RF, *n* (%)	53 (39.8)	10 (29.4)	0.851	0.356
anti-CCP, *n* (%)	36 (27.1)	6 (21.4)	0.145	0.703
AKA, *n* (%)	19 (14.3)	4 (14.8)	0.000	1.000
Abnormal ECG, *n* (%)[†]	0 (0)	5 (9.1)	12.639	<0.001

[*]Before PE diagnosis. [†]S1Q3T3. Continuous data are presented as median [Q1–Q3], and categorical data as *n* (%). ACA: Anticardiolipin antibody; AHA: Anti-histone antibodies; AIIRD: Autoimmune inflammatory rheumatic diseases; AKA: Anti-keratin antibody; ALP: Alkaline phosphatase; ALT: Alanine transaminase; ANA: Antinuclear antibody; ANuA: Anti-nucleosome antibody; AST: Aspartate aminotransferase; BNP: Brain natriuretic peptide; BUN: Blood urea nitrogen; C3: Complement 3; C4: Complement 4; CCP: Cyclic citrullinated peptide; ECG: Electrocardiogram; eGFR: Estimated glomerular filtration rate; ESR: Erythrocyte sedimentation rate; hsCRP: high sensitivity C reactive protein; IgG: Immunoglobulin G; LAC: Lupus anticoagulant; LDH: Lactate dehydrogenase; Neu: Neutrophil; PE: Pulmonary embolism; PLT: Platelets; RF: Random Forest model; TC: Triglyceride; TG: Total cholesterol; WBC: White blood cell.

patients were recorded in Table 1. The distribution pattern of the artery emboli revealed by CTPA was demonstrated in Figure 1D, which showed that more than a half of the AIIRD PE patients (55.0%) suffered from a pattern with bilateral branch involvement. Embolization of the trunk of the pulmonary artery was less common. The Figure 1E illustrates the thrombi distribution in the lower extremities in AIIRD PE patients with LEDVT, of whom 59% had intermuscular vein thrombosis, followed by popliteal vein thrombosis in 44% of patients. Thrombosis of the common femoral vein, deep femoral vein, superficial femoral vein, and posterior tibial vein also occurred.

Laboratory features and potential risk factors for PE in AIIIRD patients

Comparative analysis of selected laboratory parameters between the 60 AIIRD PE patients and 180 AIIRD non-PE patients is shown in Figure 2A. Compared with AIIRD non-PE patients, elevated levels of white blood cell, neutrophil, alanine transaminase, lactate dehydrogenase, high sensitivity C reactive protein, procalcitonin, *N*-terminal pro-brain natriuretic peptide, D-dimer and decreased levels of platelets, albumin, IgG, C4 were found in the AIIRD PE patients. The ROC curves of these individual laboratory indices are plotted in Figure 2B. It can be found that the predictive performances of most indices on the prediction of PE occurrence in AIIRD were poor. Although the AUC of D-dimer could reach 0.871, this level of accuracy proved insufficient for early and precise PE prediction, subsequently therapeutic intervention, and patient survival.

To further identify the potential risks contributing to the PE occurrences in AIIRD patients, we applied univariate LR [Figure 2C and Supplementary Table 4, http://links.lww.com/CM9/B902] and LASSO [Figure 2D] methods to screen the baseline features. Using the univariate LR approach led to the selection of 24 features, with 21 of them exhibiting a positive correlation with the occurrence of PE in AIIRD (OR >1, P <0.05) and the remaining two features exhibiting a negative correlation (OR <1, P <0.05) [Figure 2C]. The LASSO strategy yielded 13 features, of which 10 were deemed as high-risk factors for PE in AIIRD and three were categorized as low-risk factors [Figure 2D].

ML-based model training for the prediction of PE in AIIRD patients

While CTPA remains the "gold standard" for PE diagnosis, its invasiveness, reliance on available hospital equipment, and time-consuming nature pose limitations. To enhance early PE diagnosis and reduce reliance on CTPA, we employed baseline clinical laboratory parameters filtered through the univariate LR and LASSO strategies to train five ML models (SVM, RF, LR, NN, and GBDT), aiming to predict the occurrences of PE in AIIRD patients. All of these models demonstrated promising predictive performances in the training cohort. Specifically, models derived from univariate LR-selected features achieved an AUC of 1.000, 0.978, 0.962, 0.982, and 0.990 for RF, SVM, NN, LR, and GBDT, respectively [Figure 3A, left], whereas those based on LASSO-selected features yielded an AUC of 1.000, 0.993, 0.998, 0.995, and 0.992 for RF, SVM, NN, LR, and GBDT, respectively [Figure 3A, right]. The corresponding significance of the selected variables in each ML models is shown in Figure 3B. We further constructed a correlation matrix incorporating all 26 features selected by univariate LR and LASSO. This matrix offers an internal "correlation pattern" revealing indices closely associated with PE occurrences in patients with AIIRD, functioning as a potential clinical tool to heighten suspicion of PE.

Promising performance exhibited by decision trees derived from ML methods

Although all five aforementioned models showed strong predictive capabilities, given the computational intricacies, a straightforward and logical model with robust predictive performance was desired for current clinical application. Therefore, we trained the decision trees with C5.0 and CART methods, which displayed a concise and explicit risk prediction capabilities for patients with AIIRD and PE [Figure 4A]. Trees derived from the CART model trained with features selected by univariate LR and LASSO strategies were the same [Figure 4B] and only

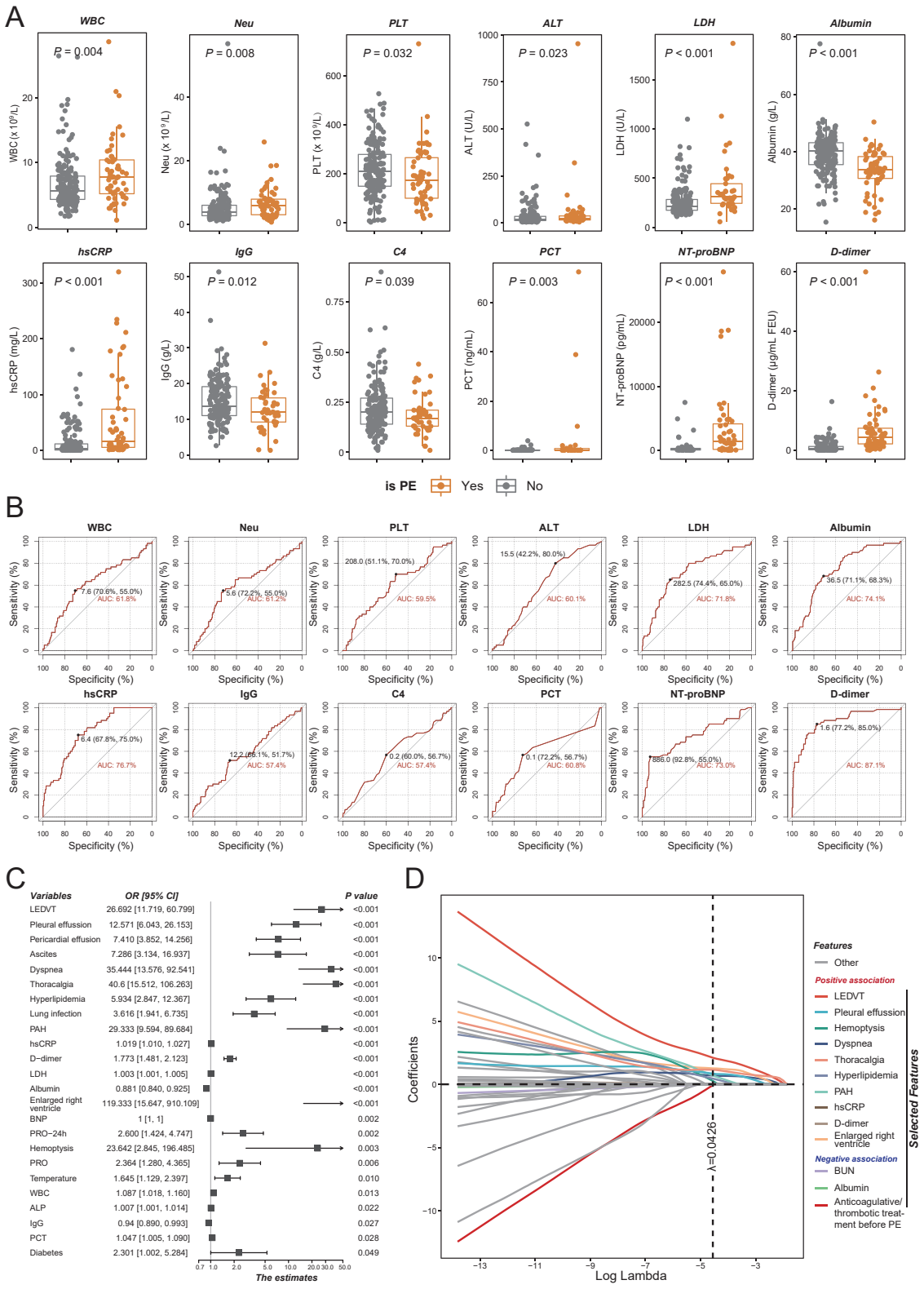

Figure 2: Statistical analysis of clinical features and feature selection by univariate LR and LASSO strategies. (A) Box and jitter plots showed distribution of continuous features between AIIRD without PE patients ($n = 180$) and AIIRD with PE patients ($n = 60$). The center line represents the median of the feature. Box limits represent upper and lower quartiles. Whiskers represent 1.5 times IQR. (B) The ROC curve showed the diagnostic efficiency of each feature. A high AUC indicates a good diagnostic performance of the corresponding feature. (C) The forest plot shows the OR values and 95% confidence intervals for 24 features selected by univariate LR. (D) LASSO variable trace profiles of baseline clinical features. The vertical dashed line shows the best lambda value, 0.0426, chosen by ten-fold cross-validation, and finally, 13 features were selected. AIIRD: Autoimmune inflammatory rheumatic diseases; ALP: Alkaline phosphatase; ALT: Alanine transaminase; AUC: Area under the ROC curve; BNP: Brain natriuretic peptide; BUN: Blood urea nitrogen; hsCRP: High sensitivity C reactive protein; IgG: Immunoglobulin G; IQR: Interquartile range; LASSO: Least absolute shrinkage and selection operator; LDH: Lactate dehydrogenase; LEDVT: Lower extremity deep vein thrombosis; LR: Logistic regression; Neu: Neutrophil count; NT-proBNP: *N*-terminal pro-brain natriuretic peptide; PAH: Pulmonary arterial hypertension; PCT: Procalcitonin; PE: Pulmonary embolism; PLT: Platelets; PRO: Urine protein; ROC: Receiver operating characteristics; WBC: White blood cell.

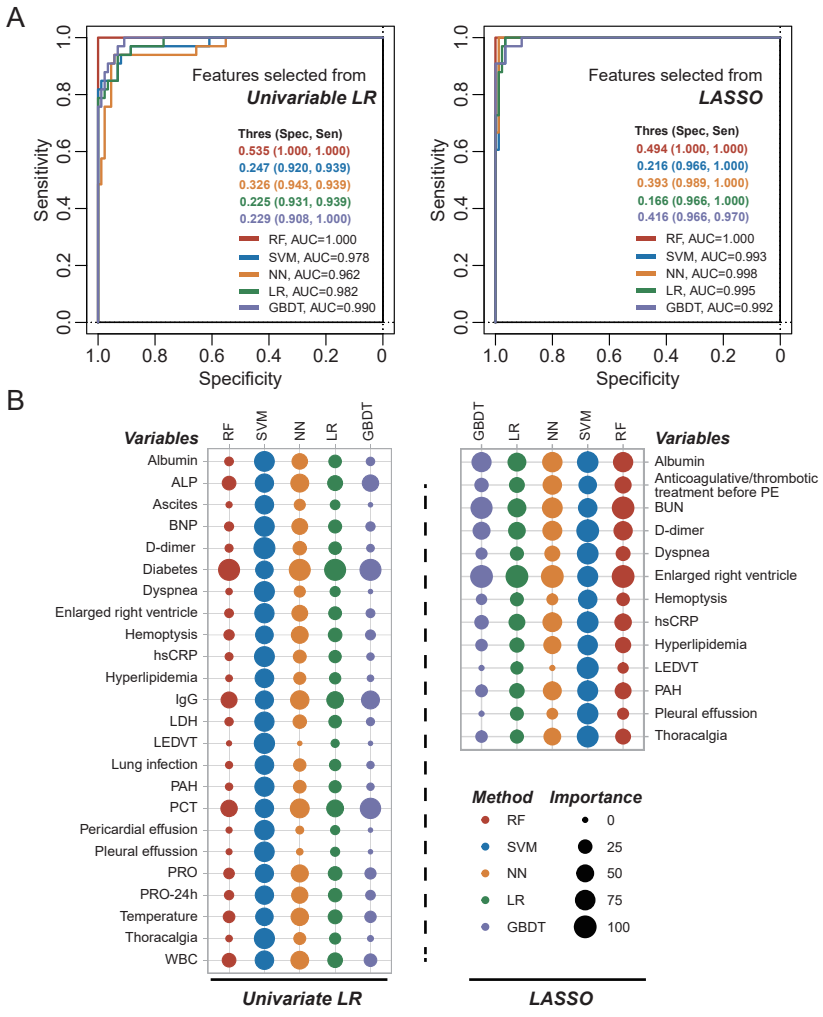

Figure 3: Model performance of five ML models for risk prediction for AIIRD with PE. (A) The ROC curves showed the diagnostic efficiency of each ML model selected by univariate LR (left) and LASSO (right), respectively. (B) Scaled importance rank of all features included in five ML models for risk prediction for AIIRD with PE. The size of circles represents the value of relative importance. The different color of circles represents the feature importance in different models. The left panel showed the features selected by univariate LR strategy; the right panel showed the features selected by LASSO strategy. AIIRD: Autoimmune inflammatory rheumatic disease; ALP: Alkaline phosphatase; AUC: Area under the ROC curve; BNP: Brain natriuretic peptide; BUN: Blood urea nitrogen; GBDT: Gradient-Boosting Decision Tree model; hsCRP: High sensitivity C reactive protein; IgG: Immunoglobulin G; LASSO: Least absolute shrinkage and selection operator; LDH: Lactate dehydrogenase; LEDVT: Lower extremity deep vein thrombosis; LR: Logistic regression; ML: Machine learning; NN: Neural Network model; PAH: Pulmonary arterial hypertension; PCT: Procalcitonin; PE: Pulmonary embolism; PRO: Urine protein; RF: Random Forest model; SVM: Support vector machine model; WBC: White blood cell.

achieved a limited predictive performance with an AUC of 0.850 [Figure 4C]. In contrast, the tree derived from C5.0 model, trained with LASSO-selected features, performed better (with an AUC of 0.932) in internal validation [Figure 4D, bottom right, and Figure 4E]. Conversely, the C5.0 model tree trained with univariate LR-selected features was intricate and displayed inferior performance compared with its LASSO counterpart. (data not shown). We further investigated the combined predictive potential of the C5.0 tree and the most predictive aforementioned individual laboratory index, D-dimer [Figure 4D]. Notably, in the training cohort, an AUC of 0.953 was achieved for PE prediction in patients with D-dimer levels exceeding upper limit of normal value. However, when solely relying on D-dimer levels for PE prediction, the sensitivity and specificity for patients with AIIRD were 96.7% and 46.2%, respectively.

It should be noted, although as the threshold elevated, higher specificity was observed when only D-dimer was applied to predict PE occurrence, its sensitivity decreased. The corresponding diagnostic procedure based solely on D-dimer levels could not adequately reflect the pathogenic logic of PE in AIIRD at the level of pathophysiology, when compared with the diagnostic procedure combining D-dimer levels and the C5.0 model.

Multicenter validation of ML-trained predictive models

We further enrolled 41 AIIRD PE cases from four centers (Zhongnan Hospital Affiliated to Wuhan University, Jingzhou Central Hospital, Hubei University for Nationalities Affiliated Hospital, and Yichang Central People's Hospital) for the multicentric validation. The baseline data of these patients are listed in Supplementary Table 5, http://links.lww.com/CM9/B902. The RF, SVM, NN, LR, and GBDT models achieved an AUC of 0.999, 0.969, 0.986, 0.969, and 0.988, respectively [Figure 5A, left]. The C5.0 tree exhibited statistically significant

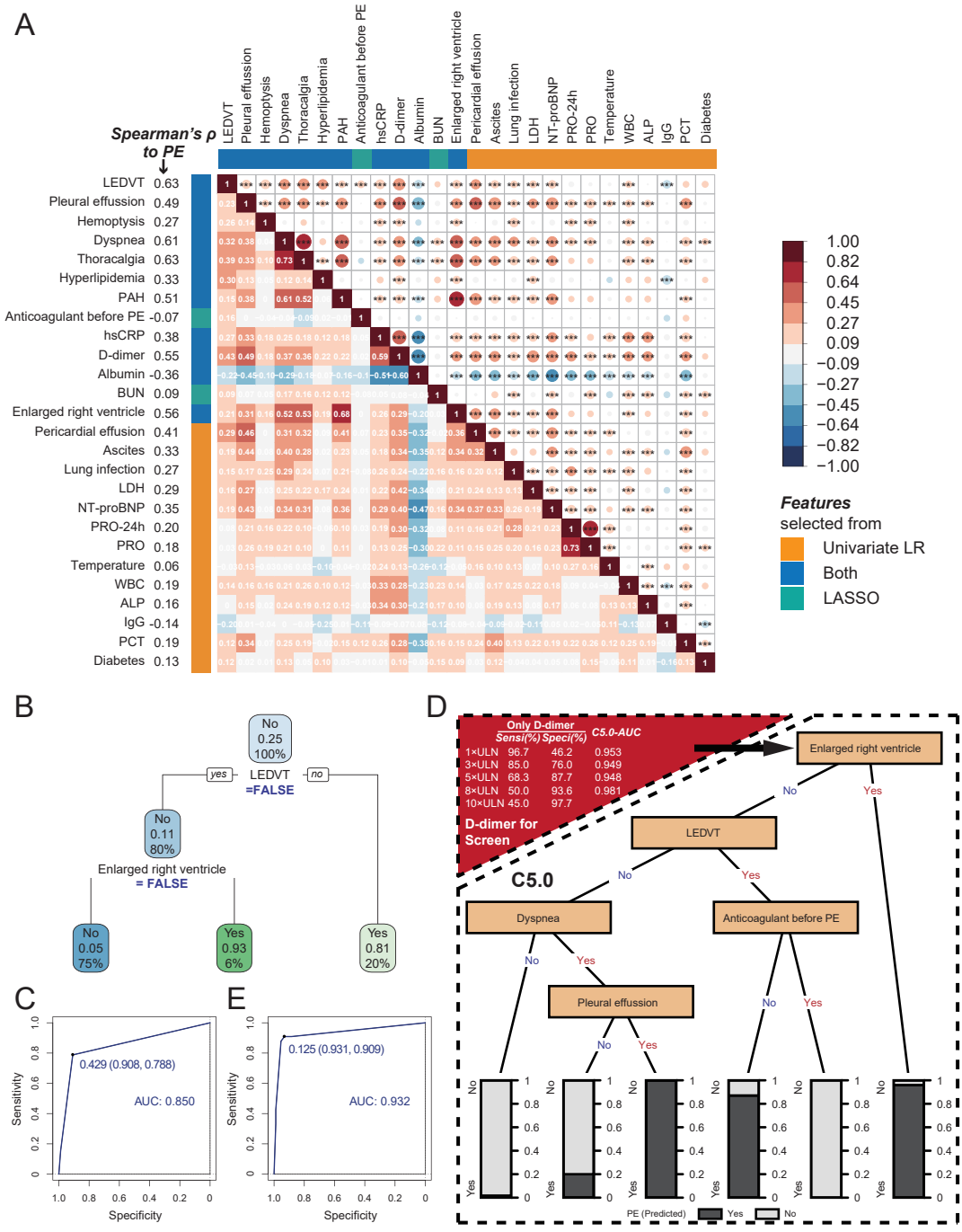

Figure 4: Correlations between features included in models and new ML model performance. (A) Spearman's correlation matrix of variables selected by LASSO and univariate LR strategies. The colors of the plot represented the correlation coefficients. A redder color represented a stronger positive monotonic relationship. A bluer color represented a stronger negative monotonic relationship. The colors of the bar represented the features by different methods. The orange, green, and blue color meant the feature was selected by univariate LR, LASSO, and both strategies, respectively. The size of the circle represents the absolute value of the correlation coefficient, where a larger circle represented a stronger correlation. The numbers in the lower triangle represented the value of correlation coefficient. (B) The decision tree diagram derived from CART model. (C) The predictive performance of CART tree, and the AUC was 0.850. (D) The C5.0 tree and its predictive performance in combination with D-dimer level or itself alone. The upper left red area represented the level of D-dimer and information of the predictive performance of D-dimer alone and in combination with C5.0 model. The bottom right region is C5.0 tree (derived from features selected by LASSO strategy). (E) The diagnostic performance of C5.0 tree alone, and the AUC was 0.932. ALP: Alkaline phosphatase; AUC: Area under the ROC curve; BUN: Blood urea nitrogen; CART: Classification and Regression Trees model; hsCRP: high sensitivity C reactive protein; IgG: Immunoglobulin G; LASSO: Least absolute shrinkage and selection operator; LDH: Lactate dehydrogenase; LEDVT: Lower extremity deep vein thrombosis; LR: Logistic Regression; ML: Machine learning; PAH: Pulmonary arterial hypertension; PCT: Procalcitonin; PRO: Urine protein; WBC: White blood cell.

superior predictive performance compared with solitary D-dimer levels, whether applied independently or in combination with the D-dimer level. [Figure 5A, right]. We further investigated the detailed performance of these ML and ML-derived models in predicting the 41 AIIRD PE patients enrolled from multiple centers [Figure 5B]. The majority of PE occurrences were identified by all six algorithms, and the prediction of PE occurrence reached 100% when all six algorithms were concurrently applied.

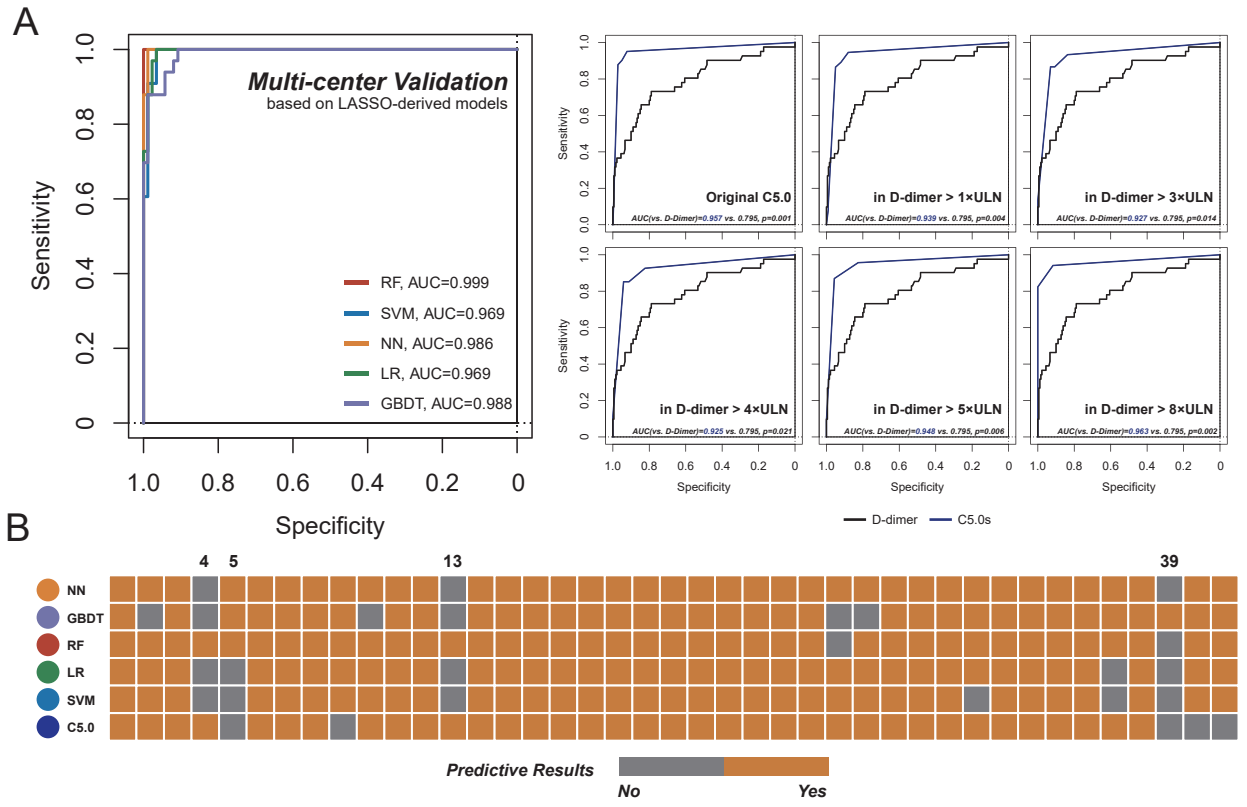

Figure 5: Performance of the ML models/ML-derived tree with multicentric data. (A) 41 AIIRD PE cases for validation were collected from four different centers. The left panel of the ROC curves showed the predictive performances of five ML models based on LASSO selected features on the validation cohort; the right panel of the ROC curves showed the predictive performances of original C5.0 tree and D-dimer combined C5.0 tree (dark blue line). The ROC curve of D-dimer alone in the validation cohort was plotted with "black line". (B) Heatmap showed the detailed predictive performance by the 6 ML models/ML-derived tree. Each square represented one single case in these 41 AIIRD PE patients. Patients who were able to be identified by the corresponding predictive model were marked in orange; others were in gray. AIIRD: Autoimmune inflammatory rheumatic disease; AUC: Area under the ROC curve; GBDT: Gradient boosted decision tree; LASSO: Least absolute shrinkage and selection operator; LR: Logistic regression; ML: Machine learning; NN: Neural network; PE: Pulmonary embolism; RF: Random forest; ROC: Receiver operating characteristics; SVM: Support vector machine.

Discussion

PE, a frequent and life-threatening acute cardiovascular syndrome, presents an annual incidence of 0.38 per 1000 individuals in the general population.[23] Within Tongji Hospital, the rate of PE among AIIRD patients is 0.827%, accompanied by a mortality rate of 8.22%. The challenge of accurately and promptly identifying PE occurrences arises from the absence of specific clinical signs and symptoms, leading to unfavorable prognoses. Early prediction and timely intervention in reducing mortality rates are crucial. While imaging (e.g., CTPA) tests are common for diagnosis, they are often feasible for almost all suspected cases. Moreover, radiological examinations take considerable time. Several prediction systems have been developed to predict the onset of PE. The most frequently used predictive systems are the Geneva rule, the Wells rule, and their simplified versions.[24–27] Despite their routine use, only approximately 8% of patients in US emergency departments and 27% in Europe have been confirmed using these scoring systems.[28] Moreover, these systems include certain items that are unsuitable for AIIRD patients, such as surgical history, fractures, and active cancer. Previous studies on PE in AIIRD patients have only evaluated the risk factors for PE, without offering convenient or rapid methods for early and accurate prediction of PE in AIIRD patients.[29,30] The demand for practical risk assessment systems that are specific for recognizing PE in AIIRD patients remains urgent. In light of the vast and intricate clinical data generated today, diagnostic algorithms stemming from subjective physician experience or conventional statistical methods often fall short of delivering exceptional performance. In response, we conceived this multicenter study, training multiple ML models to facilitate precise and convenient prediction of PE occurrence in AIIRD patients without relying on CTPA examinations. Impressively, all these models demonstrated encouraging predictive capabilities. This affirms that ML-based models can substantially enhance the efficiency of predicting specific pathophysiological conditions, providing substantial assistance to physicians in finalizing diagnoses. This direction aligns with the future trend of early and accurate diagnosis and risk prediction in clinical practice. However, most of these ML models currently necessitate computer assistance, potentially inconveniencing physicians, especially in scenarios where suitable computing equipment is unavailable. To provide a high-performance and physician-friendly algorithm, we obtained the decision trees trained through CART and C5.0 methods. Notably, the C5.0 tree trained with features selected by LASSO strategy demonstrated robust predictive performance while maintaining a relatively simple structure, thus offering a practical tool for physicians.

The nodes in the C5.0 tree were related to several significant clinical features that could be elucidated within the context of the pathophysiology of PE. RV enlargement, a prevalent visual manifestation of RV overload or dysfunction in patients with PE, is identifiable in ≥25% of PE cases via transthoracic echocardiography and is linked with an unfavorable prognosis.[31,32] Our study highlighted that 57% of patients with AIIRD and PE suffered from RV enlargement, a ratio significantly surpassing that of non-PE patients with AIIRD. RV enlargement is postulated to be a sensitive marker for predicting PE,[33] which was also confirmed using the univariate LR and LASSO analyses in this study. Echocardiography used to detect RV pressure overload or dysfunction, is recommended as a diagnostic tool for these suspected high-risk PE patients with hemodynamical instability.[34] Given that RV pressure overload and dysfunction are commonly observed in acute PE, the identification of RV enlargement or dysfunction can expedite the conclusive diagnosis of PE in patients with suspected PE.[35] In the C5.0 tree, the differentiation based on RV enlargement stands as the foremost node in the entire decision tree, and the presence of RV enlargement can almost directly signal PE occurrence in patients with AIIRD.

The majority of PE originates from DVT in the lower limbs. LEDVT is regarded as a major cause of PE, with a high positive predictive value for PE.[36,37] Approximately, 40% of patients with DVT have asymptomatic PE. It is recommended that a clinical suspected patient should accept the diagnosis of PE, if the compression ultrasonography shows a proximal DVT.[34] In this study, we found that 61% of acute PE patients with AIIRD had LEDVT, with intermuscular and popliteal veins being the most common sites of LEDVT formation. The second node of the whole C5.0 tree was for distinguishing the presence of LEDVT: in AIIRD patients with clinical suspicion of PE, presence of LEDVT without previous anti-coagulant/thrombotic treatment is a high-performance predictor of PE occurrence. In addition, this reveals the importance of the anti-coagulant/thrombotic treatment for preventing further PE onset in patients with LEDVT.

Dyspnea, which is regarded as one of the most common symptoms in clinical settings, is highly related to pulmonary vascular obstruction and/or its consequences. In general, dyspnea has an acute and severe presentation in patients with central PE; in contrast, it is often mild and may be transient in patients with small peripheral PE.[34] A systematic review and meta-analysis have reported that clinical symptoms have limited diagnostic value; however, the absence of dyspnea is one of the most useful clinical features for ruling out PE.[38] In patients with preexisting heart failure or pulmonary disease, aggravating dyspnea can be the unique symptom indicator of PE. During PE diagnosis, pleural effusion is often ignored by clinicians; however, PE is responsible for quite a number of undiagnosed pleural effusions.[39] A retrospective study has reported that pleural effusion occurred in 57.01% of patients with acute PE.[40] Furthermore, dyspnea is present in more than 70% of patients with PE and pleural effusion.[39] In univariate LR analysis of PE occurrence in the present study, the ORs for dyspnea and pleural effusion, two of the most remarkable variables, were 35.444 and 12.571, respectively. The co-existence of these two variables is a very strong positive indicator of PE occurrence in AIIRD patients. Nevertheless, dyspnea without pleural effusion may have a very low clinical implication for PE prediction.

D-dimer, a laboratory index, should be discussed in the context of PE. D-dimer levels are elevated in most patients with acute PE. Therefore, it is considered a vital parameter for diagnosing venous thromboembolism (VTE) and is routinely used to identify patients at high risk of PE.[41,42] The International Medical Prevention Registry on Venous Thromboembolism (IMPROVE) risk assessment model has been comprehensively validated in patients.[43–45] The prognostic value of identifying patients at risk of developing venous thromboembolism can be improved by incorporating D-dimer with this model.[46] However, D-dimer levels can increase in various pathophysiological conditions (e.g., surgery, pregnancy, malignancy, chronic inflammatory conditions, etc.); furthermore, a small set of patients with PE have normal D-dimer levels during PE onset.[47] Therefore, only D-dimer levels alone cannot be a specific predictor or exclusive index for PE occurrence in AIIRD patients. However, when the D-dimer index is combined with C5.0 decision tree, the new algorithm increased specificity in predicting the PE occurrence and demonstrated better performance, with an AUC of 0.948–0.981 in internal validation and 0.925–0.963 in multicentric validation. Furthermore, the better performance of C5.0 tree when combined with the D-dimer is also interpretable at the pathophysiological level. As mentioned previously, abnormal D-dimer levels are an important phenomenon tightly correlated with thrombus formation. For example, in addition to PE, RV enlargement is observed in other disease conditions, including primary pulmonary hypertension (PAH). However, Can *et al*'s[48] study showed that the D-dimer levels are in the normal range (0.42 ± 0.31, ranging from 0.29 to 0.61 mg/L) in most PAH patient. Therefore, the combination of significantly increased D-dimer levels, and RV enlargement can strongly indicate PE occurrence.

The performances of our models were further validated by multicentric data. The AUCs of all five ML models (RF, SVM, NN, LR, and GBDT) trained with features selected by LASSO strategy were more than 0.96, ranging from 0.969 to 0.999. The ML-derived C5.0 tree algorithm performed well (significantly better than D-dimer levels alone). It should be noted that although no single method (namely, ML models or ML-derived tree algorithms) alone can perfectly identify all the PE cases in our study; the multicentric PE cases can be recognized by at least one method. Therefore, a combination of the predictive results of these methods can achieve fascinating performance.

To date, no ML-based scoring system is available for predicting the occurrence of AIIRD patients with acute PE. ML is thought to be a potential tool of promoting the efficiency. In addition to describing the contributions of features to the outcomes, in the present study, we also extracted significant clinical features from the original clinical data and established many high-performance

models and a simple and practical predictive model using ML methods; this model not only indicated the development orientation of accurate diagnosis but also provided a convenient algorithm for clinical applications in current settings. With these algorithms, clinicians can timely predict and categorize these AIIRD patients at risk for PE without the CTPA results, hopefully improving patients' prognosis. Furthermore, these algorithms provide an approach for clinicians to promptly identify and stratify the risk of PE in AIIRD patients, particularly critical patients.

The present study has some limitations: First, 180 AIIRD non-PE cases were used in both training and validation cohort. Choosing more new non-PE patients matched with the 41 AIIRD PE patients from multiple centers for validation will be better. Second, owing to the limitations of a retrospective study, some missing values are inevitable. Therefore, prospective studies should be conducted to acquire complete data. Third, although we trained these models and validated their performance with multicentric data, our study is retrospective, and the number of patients enrolled in remains limited. Therefore, the performance of these models should be further validated both retrospectively and prospectively using large-scale multicentric cohorts.

In conclusion, in the present study, we revealed that ML-based models can accurately predict the occurrence of PE in AIIRD patients with clinical suspicion of PE. We not only provided a convenient algorithm for current clinical applications in PE prediction (in AIIRD patients) but also highlighted the potential of ML methods in achieving an accurate diagnosis.

Acknowledgement

The authors would like to thank all patients participated in this study.

Funding

This work was supported by grants from National Natural Science Foundation of China (Nos. 81703058 and 81974254) and Tongji Hospital Clinical Research Flagship Program (No. 2019CR206).

Conflicts of interest

None.

References

1. Goldhaber SZ, Elliott CG. Acute pulmonary embolism: Part I: Epidemiology, pathophysiology, and diagnosis. Circulation 2003;108:2726–2729. doi: 10.1161/01.CIR.0000097829.89204.0C.
2. Goldhaber SZ, Visani L, De Rosa M. Acute pulmonary embolism: Clinical outcomes in the International Cooperative Pulmonary Embolism Registry (ICOPER). Lancet 1999;353:1386–1389. doi: 10.1016/s0140-6736(98)07534-5.
3. Laporte S, Mismetti P, Décousus H, Uresandi F, Otero R, Lobo JL, *et al*. Clinical predictors for fatal pulmonary embolism in 15,520 patients with venous thromboembolism: Findings from the Registro Informatizado de la Enfermedad TromboEmbolica venosa (RIETE) Registry. Circulation 2008;117:1711–1716. doi: 10.1161/CIRCULATIONAHA.107.726232.
4. Wang ZL. Acute pulmonary embolism: The clinical conundrum. Chin Med J 2012;125:352–366.
5. Lee YJ, Zakaria R, Manaf ZA, Mohamed Z, Lee YY. Value of CT pulmonary arteriography and venography in the evaluation of venous thromboembolism in a multiracial Asian population. Chin Med J 2013;126:2049–2053.
6. Li L, Lu N, Avina-Galindo AM, Zheng Y, Lacaille D, Esdaile JM, *et al*. The risk and trend of pulmonary embolism and deep vein thrombosis in rheumatoid arthritis: A general population-based study. Rheumatology (Oxford) 2021;60:188–195. doi: 10.1093/rheumatology/keaa262.
7. Zöller B, Li X, Sundquist J, Sundquist K. Risk of pulmonary embolism in patients with autoimmune disorders: A nationwide follow-up study from Sweden. Lancet 2012;379:244–249. doi: 10.1016/S0140-6736(11)61306-8.
8. Aviña-Zubieta JA, Vostretsova K, De Vera MA, Sayre EC, Choi HK. The risk of pulmonary embolism and deep venous thrombosis in systemic lupus erythematosus: A general population-based study. Semin Arthritis Rheum 2015;45:195–201. doi: 10.1016/j.semarthrit.2015.05.008.
9. Aviña-Zubieta JA, Jansz M, Sayre EC, Choi HK. The risk of deep venous thrombosis and pulmonary embolism in primary Sjögren syndrome: A general population-based study. J Rheumatol 2017;44:1184–1189. doi: 10.3899/jrheum.160185.
10. Carruthers EC, Choi HK, Sayre EC, Aviña-Zubieta JA. Risk of deep venous thrombosis and pulmonary embolism in individuals with polymyositis and dermatomyositis: A general population-based study. Ann Rheum Dis 2016;75:110–116. doi: 10.1136/annrheumdis-2014-205800.
11. Annangi S, Dammalapati TR, Nutalapati S, Henriques King MN. Prevalence of pulmonary embolism among systemic lupus erythematosus discharges: A decade of analysis of the national hospital discharge survey. J Clin Rheumatol 2017;23:200–206. doi: 10.1097/RHU.0000000000000521.
12. Schoenfeld SR, Choi HK, Sayre EC, Aviña-Zubieta JA. Risk of pulmonary embolism and deep venous thrombosis in systemic sclerosis: A general population-based study. Arthritis Care Res (Hoboken) 2016;68:246–253. doi: 10.1002/acr.22673.
13. Van Calster B, Wynants L. Machine learning in medicine. N Engl J Med 2019;380:2588. doi: 10.1056/NEJMc1906060.
14. Peiffer-Smadja N, Rawson TM, Ahmad R, Buchard A, Georgiou P, Lescure FX, *et al*. Machine learning for clinical decision support in infectious diseases: A narrative review of current applications. Clin Microbiol Infect 2020;26:584–595. doi: 10.1016/j.cmi.2019.09.009.
15. Greener JG, Kandathil SM, Moffat L, Jones DT. A guide to machine learning for biologists. Nat Rev Mol Cell Biol 2022;23:40–55. doi: 10.1038/s41580-021-00407-0.
16. Xue B, Li D, Lu C, King CR, Wildes T, Avidan MS, *et al*. Use of machine learning to develop and evaluate models using preoperative and intraoperative data to identify risks of postoperative complications. JAMA Netw Open 2021;4:e212240. doi: 10.1001/jamanetworkopen.2021.2240.
17. Sherman E, Alejo D, Wood-Doughty Z, Sussman M, Schena S, Ong CS, *et al*. Leveraging machine learning to predict 30-day hospital readmission after cardiac surgery. Ann Thorac Surg 2022;114:2173–2179. doi: 10.1016/j.athoracsur.2021.11.011.
18. Yan X, Goldsmith J, Mohan S, Turnbull ZA, Freundlich RE, Billings FT 4th, *et al*. Impact of intraoperative data on risk prediction for mortality after intra-abdominal surgery. Anesth Analg 2022;134:102–113. doi: 10.1213/ANE.0000000000005694.
19. Harris AHS, Trickey AW, Eddington HS, Seib CD, Kamal RN, Kuo AC, *et al*. A tool to estimate risk of 30-day mortality and complications after hip fracture surgery: Accurate enough for some but not all purposes? A study from the ACS-NSQIP database. Clin Orthop Relat Res 2022;480:2335–2346. doi: 10.1097/CORR.0000000000002294.
20. Vollmer S, Mateen BA, Bohner G, Király FJ, Ghani R, Jonsson P, *et al*. Machine learning and artificial intelligence research for patient benefit: 20 critical questions on transparency, replicability, ethics, and effectiveness. BMJ 2020;368:l6927. doi: 10.1136/bmj.l6927.
21. Carracedo-Reboredo P, Liñares-Blanco J, Rodríguez-Fernández N, Cedrón F, Novoa FJ, Carballal A, *et al*. A review on machine learning approaches and trends in drug discovery. Comput Struct Biotechnol J 2021;19:4538–4558. doi: 10.1016/j.csbj.2021.08.011.

22. Hosseini MP, Hosseini A, Ahi K. A review on machine learning for EEG signal processing in bioengineering. IEEE Rev Biomed Eng 2021;14:204–218. doi: 10.1109/RBME.2020.2969915.
23. Alotaibi GS, Wu C, Senthilselvan A, McMurtry MS. Secular trends in incidence and mortality of acute venous thromboembolism: The AB-VTE population-based study. Am J Med 2016;129:879.e19–e25. doi: 10.1016/j.amjmed.2016.01.041.
24. Wells PS, Anderson DR, Rodger M, Ginsberg JS, Kearon C, Gent M, *et al*. Derivation of a simple clinical model to categorize patients probability of pulmonary embolism: Increasing the models utility with the SimpliRED D-dimer. Thromb Haemost 2000;83:416–420. doi: 10.1055/s-0037-1613830.
25. Klok FA, Mos IC, Nijkeuter M, Righini M, Perrier A, Le Gal G, *et al*. Simplification of the revised Geneva score for assessing clinical probability of pulmonary embolism. Arch Intern Med 2008;168:2131–2136. doi: 10.1001/archinte.168.19.2131.
26. Gibson NS, Sohne M, Kruip MJ, Tick LW, Gerdes VE, Bossuyt PM, *et al*. Further validation and simplification of the Wells clinical decision rule in pulmonary embolism. Thromb Haemost 2008;99:229–234. doi: 10.1160/TH07-05-0321.
27. Douma RA, Mos IC, Erkens PM, Nizet TA, Durian MF, Hovens MM, *et al*. Performance of 4 clinical decision rules in the diagnostic management of acute pulmonary embolism: A prospective cohort study. Ann Intern Med 2011;154:709–718. doi: 10.7326/0003-4819-154-11-201106070-00002.
28. Kline JA. Utility of a clinical prediction rule to exclude pulmonary embolism among low-risk emergency department patients: Reason to PERC up. JAMA 2018;319:551–553. doi: 10.1001/jama.2017.21901.
29. You H, Zhao J, Wang Q, Tian X, Li M, Zeng X. Characteristics and risk factors of pulmonary embolism in patients with systemic lupus erythematosus: A case control study. Clin Exp Rheumatol 2020;38:940–948.
30. Burgos PI, McGwin G Jr., Reveille JD, Vilá LM, Alarcón GS. Factors predictive of thrombotic events in LUMINA, a multi-ethnic cohort of SLE patients (LXXII). Rheumatology (Oxford) 2010;49:1720–1725. doi: 10.1093/rheumatology/keq140.
31. Kurnicka K, Lichodziejewska B, Goliszek S, Dzikowska-Diduch O, Zdończyk O, Kozłowska M, *et al*. Echocardiographic pattern of acute pulmonary embolism: Analysis of 511 consecutive patients. J Am Soc Echocardiogr 2016;29:907–913. doi: 10.1016/j.echo.2016.05.016.
32. Pruszczyk P, Goliszek S, Lichodziejewska B, Kostrubiec M, Ciurzyński M, Kurnicka K, *et al*. Prognostic value of echocardiography in normotensive patients with acute pulmonary embolism. JACC Cardiovasc Imaging 2014;7:553–560. doi: 10.1016/j.jcmg.2013.11.004.
33. Singh S, Lewis MI. Evaluating the right ventricle in acute and chronic pulmonary embolism: Current and future considerations. Semin Respir Crit Care Med 2021;42:199–211. doi: 10.1055/s-0040-1722290.
34. Konstantinides SV, Meyer G, Becattini C, Bueno H, Geersing GJ, Harjola VP, *et al*. 2019 ESC Guidelines for the diagnosis and management of acute pulmonary embolism developed in collaboration with the European Respiratory Society (ERS). Eur Heart J 2020;41:543–603. doi: 10.1093/eurheartj/ehz405.
35. Alerhand S, Sundaram T, Gottlieb M. What are the echocardiographic findings of acute right ventricular strain that suggest pulmonary embolism? Anaesth Crit Care Pain Med 2021;40:100852. doi: 10.1016/j.accpm.2021.100852.
36. Qiu T, Zhang T, Liu L, Li W, Li Q, Zhang X, *et al*. The anatomic distribution and pulmonary embolism complications of hospital-acquired lower extremity deep venous thrombosis. J Vasc Surg Venous Lymphat Disord 2021;9:1391–1398.e3. doi: 10.1016/j.jvsv.2021.03.004.
37. Le Gal G, Righini M, Sanchez O, Roy PM, Baba-Ahmed M, Perrier A, *et al*. A positive compression ultrasonography of the lower limb veins is highly predictive of pulmonary embolism on computed tomography in suspected patients. Thromb Haemost 2006;95:963–966. doi: 10.1160/TH06-03-0158.
38. West J, Goodacre S, Sampson F. The value of clinical features in the diagnosis of acute pulmonary embolism: Systematic review and meta-analysis. QJM 2007;100:763–769. doi: 10.1093/qjmed/hcm113.
39. Findik S. Pleural effusion in pulmonary embolism. Curr Opin Pulm Med 2012;18:347–354. doi: 10.1097/MCP.0b013e32835395d5.
40. Zhang J, Zhou H, Aili A, Wang M, Shen Y, Yi Q. Prevalence and clinical significance of pleural effusion in patients with acute pulmonary embolism: A retrospective study. J Thorac Dis 2021;13:541–551. doi: 10.21037/jtd-20-2552.
41. Wang J, Wu XY, Liang Y, Guo W. Predictive value of the Wells score combined with D-dimer level in identifying acute pulmonary embolism in patients with coronary heart disease with chest pain. Chin Med J 2020;133:2253–2255. doi: 10.1097/CM9.0000000000000988.
42. Guo DJ, Zhao C, Zou YD, Huang XH, Hu JM, Guo L. Values of the Wells and revised Geneva scores combined with D-dimer in diagnosing elderly pulmonary embolism patients. Chin Med J 2015;128:1052–1057. doi: 10.4103/0366-6999.155085.
43. Spyropoulos AC, Anderson FA Jr, FitzGerald G, Decousus H, Pini M, Chong BH, *et al*. Predictive and associative models to identify hospitalized medical patients at risk for VTE. Chest 2011;140:706–714. doi: 10.1378/chest.10-1944.
44. Greene MT, Spyropoulos AC, Chopra V, Grant PJ, Kaatz S, Bernstein SJ, *et al*. Validation of risk assessment models of venous thromboembolism in hospitalized medical patients. Am J Med 2016;129:1001.e9–1001.e18. doi: 10.1016/j.amjmed.2016.03.031.
45. Rosenberg D, Eichorn A, Alarcon M, McCullagh L, McGinn T, Spyropoulos AC. External validation of the risk assessment model of the International Medical Prevention Registry on Venous Thromboembolism (IMPROVE) for medical patients in a tertiary health system. J Am Heart Assoc 2014;3:e001152. doi: 10.1161/JAHA.114.001152.
46. Gibson CM, Spyropoulos AC, Cohen AT, Hull RD, Goldhaber SZ, Yusen RD, *et al*. The IMPROVEDD VTE risk score: Incorporation of D-dimer into the IMPROVE score to improve venous thromboembolism risk stratification. TH Open 2017;1:e56–e65. doi: 10.1055/s-0037-1603929.
47. Guo Z, Ma Q, Zheng Y, Zhang Y, Ge H. Normal blood D-dimer concentrations: Do they exclude pulmonary embolism? Chin Med J 2014;127:18–22.
48. Can MM, Tanboğa IH, Demircan HC, Ozkan A, Koca F, Keleş N, *et al*. Enhanced hemostatic indices in patients with pulmonary arterial hypertension: An observational study. Thromb Res 2010;126:280–282. doi: 10.1016/j.thromres.2010.06.020.

How to cite this article: Hu ZW, Hu YY, Zhang SQ, Dong L, Chen XQ, Yang HQ, Su LC, Hou XQ, Huang X, Shen XL, Ye C, Tu W, Chen Y, Chen YX, Cai SZ, Zhong JX, Dong LL. Machine-learning-based models assist the prediction of pulmonary embolism in autoimmune diseases: A retrospective, multicenter study. Chin Med J 2024;137:1811–1822. doi: 10.1097/CM9.0000000000003025